

IMITATION ANALYSIS OF CREMATION FURNACE HEAT TRANSFER UNDER THE FINITE ELEMENT SIMULATION SOFTWARE

by

Jingyun JIA*, Xiaolong ZOU, Xiantao CHEN,
Haibin WANG, and Qiang SUN

Civil Aviation Flight University of China, Guanghan, Sichuan, China

Original scientific paper
<https://doi.org/10.2298/TSCI191216127J>

To promote the full combustion efficiency of a body cremation furnace during cremation, the temperature and velocity of cremation furnace in the process of body combustion are simulated by finite element model. Firstly, the simplified finite element analysis model of cremation furnace and its finite element software is introduced in this study, and then the flow model, heat transfer model, and combustion model needed in the heat transfer process are described. According to the requirements of the finite element model, the mesh generation process of the cremation furnace model and the numerical solution method are presented. Finally, the model used in this study is verified by the test and simulation results. The results show that the method is reliable. Besides, the design parameters of the temperature part and the combustion speed part of the furnace under six different working conditions are analyzed to further optimize the structure of the furnace. The results of this study provide a good theoretical basis for cremation equipment and promote the development of China's cremation industry.

Key words: finite element, cremator, flow model, heat transfer model, combustion model

Introduction

With the change of times and people's cognition, cremation is chosen instead of burial by a growing number of people. There are three main aspects for this change in perception. Firstly: with the development of economy, the rural land area is less, and there is no extra land for burial. Secondly: the ashes are stored after cremation, which is convenient for sacrifice. Thirdly: the infectious diseases are prevented, and cremation is the main way of body disposal in China [1].

However, with the aggravation of environmental pollution, a series of environmental protection laws and regulations and related standards are published in China, and the requirements for smoke emissions becomes stringent. Therefore, it is necessary to design and improve the structure of the cremation furnace, and the national environmental requirements are met [2]. The combustion in the furnace chamber is determined by the structure of the cremation furnace, and the effect of the cremation of body is decided by the combustion in the furnace chamber. In the process of cremation, the cremation effect of the body is not only affected by the size and shape of the interior of the furnace, but also by various internal and external factors such as the

* Corresponding author, e-mail: 1712431697@qq.com

pressure of combustion gas, temperature, and air supply. The size of chemical reaction rate in the combustion process is affected by the change of each parameter. Moreover, during the combustion process, the reflux area and turbulence intensity formed in the furnace is also influenced by it, thus the whole combustion process is affected [3]. In general, it is difficult to test turbulence in the furnace during cremation, and the velocity field in the furnace is comprehended on the basis of the black box model. The parameter design of the technical scheme of cremation equipment is mainly depended on the empirical data, which is less scientific and accurate. In recent years, with the development of computer science and fluid mechanics, commercial CFD software is widely used [4]. The computer simulation technology of incineration process is mature. The defect that all similar conditions cannot be satisfied in physical simulation is well avoided by the computer simulation. It has the advantages of easy to change operation parameters and easy to control boundaries, and is applied in many practical projects [5].

In summary, to study the heat transfer mode of the body cremation furnace, the finite element analysis method is adopted in this study. Firstly, the object of this study and the simplified process under the finite element model are introduced, and the related models of heat transfer (flow model, heat transfer model, and combustion model) are described in detail. Then, the meshing of the finite element model and the numerical solution method are presented. Finally, the simplified model in this study is verified through the actual measured value and the simulated value. Six different working conditions are designed to simulate the structure of the cremation furnace and optimize the design parameters of the furnace. Therefore, a good theoretical basis is provided for the optimization of cremation equipment.

Methodology

Simplification of research object and model

The object of this study is the cremation furnace. The burning of remains is carried out in the cremation furnace, but the cremation process of remains is complicated. This complexity is reflected in two aspects. Elemental analysis of the remains is needed before cremation. Through the analysis of elemental, varieties of gases are produced by the body during combustion, combustible gases are also included. During the volatilization process, the body is reacted with the surrounding air to produce non-volatile solids, such as the reaction of coke with oxidizer. Therefore, there is a three-phase reaction in the combustion process. The shape of the body surface is complex, and the shape of the body surface is changed with the combustion, thus the surface in contact with the gas is altered in real time [6, 7].

In this study, the complexity of cremation is simplified considering the computational objective. First of all, an area is divided at the bottom of the furnace chamber to describe the combustion process of the body in the furnace chamber, then the exchange of the body in the region with the surrounding material and the material in the furnace chamber is realized. In this study, the boundary conditions of the combustion zone are set as functions that change over time. The process is divided into three steps: the first step is that at the initial stage, the temperature in the combustion zone is relatively low, and the heat absorption is generated to the outside world, while the conditions set on the wall of the cremation furnace are heat absorption. In the second step, when a range of 400~600 K is reached by the temperature in the combustion zone and a certain value is remained, volatilization is occurred in the combustion zone, volatilization begins to precipitate, and the volatilization absorbs heat. At this point, the wall condition of the cremation furnace remains endothermic (but the endothermic rate in the second step is much higher than that in the first step). Thirdly, after volatilization, combustible gas and solid begin to

burn. Combustible components are outputted to the surrounding area by combustion zone. At this time, the wall condition of the cremation furnace is set as the entrance of combustible.

The cremator currently used in funeral homes is taken as the physical prototype in this study, then the calculation model is achieved according to the simplified processing process, as shown in fig. 1.

Flow model heat transfer model and combustion model are introduced

The governing equation of the combustion process of the body in the cremation furnace is composed of turbulence model equation, heat transfer model equation, and combustion model equation. Therefore, the equations involved in the cremation process is described in this study [8, 9].

In the combustion process, the mass conservation expression is:

$$\frac{\partial \rho}{\partial t} + \nabla(\rho \bar{v}) = 0 \tag{1}$$

where ∇ is the degree of dispersion, ρ [kgm⁻³] – the density of the fluid, t [s] – the time, and \bar{v} [ms⁻¹] – the velocity vector.

Expression of ∇ is:

$$\nabla a = \text{div}(a) = \frac{\partial a_x}{\partial x} + \frac{\partial a_y}{\partial y} + \frac{\partial a_z}{\partial z} \tag{2}$$

The momentum conservation law in the combustion process is:

$$\frac{\partial \rho}{\partial t}(\rho \bar{v}) = \nabla(\rho \bar{v} \bar{v}) = -\nabla p + \nabla(\bar{\tau}) + \rho \bar{g} + \bar{F} \tag{3}$$

where p is the pressure on the fluid element, $\bar{\tau}$ [N] – the viscous stress on the surface of the element caused by the molecular viscosity.

The momentum conservation law in the combustion process is:

$$\frac{\partial(\rho T)}{\partial t} + \nabla(\rho u T) = \nabla \left(\frac{k}{c_p} \text{grad} T \right) + S_T \tag{4}$$

where T [K] is the local temperature, k – the heat transfer coefficient of the fluid, S_T – the viscous dissipation term, and c_p – the specific heat capacity at constant pressure.

Turbulent model

During the process of cremation, there is turbulent flow field in the combustion space of cremation furnace. The description of turbulent flow field is very complicated, and turbulence models commonly adopted include realizable k - ϵ model, standard k - ϵ , renormalization group (RNG) k - ϵ model, k - ω model, reynolds stress model (RSM), and large eddy simulation (LES) model. Therefore, in the aforementioned model, each model is applied in a different scenario, and time is seriously consumed by RSM and LES models in the calculation process. The k - ω is applicable to the problem of rotating turbulent field, and the k - ϵ is adopted to free shear flow with relatively small pressure gradient. Through the actual situation of body incin-

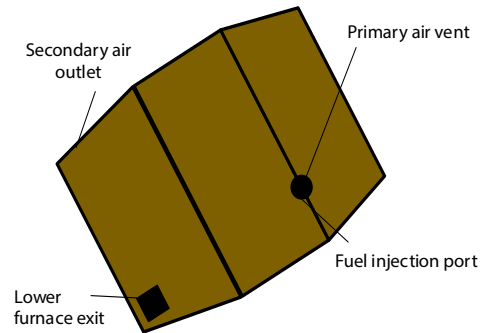


Figure 1. Calculation model of total furnace

eration, $k-\varepsilon$ model is selected to calculate the turbulent flow field in this study. Among the three $k-\varepsilon$ models mentioned previously, the realizable $k-\varepsilon$ model was selected in this study due to the shortcomings of the standard $k-\varepsilon$, RNG $k-\varepsilon$ model, and $k-\omega$ model in the calculation of turbulent flow field [10, 11].

The CFD software FLUENT6.3 is adopted to simulate the flow and combustion information in the cremation furnace. The FLUENT is a widely used fluid computing software for calculating flow fields of various complex geometric shapes, and it has a large number of widely validated models for selection.

Heat transfer model

In this study, FLUENT6.3 software in the finite element is selected to calculate the heat transfer of heat conduction and thermal convection:

$$\frac{\partial}{\partial t}(\rho E) + \nabla[v(\rho E + \rho)] = \nabla \left[k_{\text{eff}} \nabla T - \sum_j h_j \vec{J}_j + (\bar{k}_{\text{eff}} \bar{v}) \right] + S_h \quad (5)$$

where S_h is source. The heat generated by the absorption (discharge) of heat and other user-defined volumetric heat sources during chemical reactions, E – the capacity of a unit of mass, \bar{k}_{eff} – the effective thermal conductivity, and \vec{J}_j – the diffusion flux of component j .

There is radiation from high temperature flame to the wall in the combustion process of cremation furnace, thus the radiation heat transfer plays a major role in this process, and the influence of radiation on heat transfer is taken into account in the calculation process. Due to the calculation time and large optical thickness in the combustion chamber, P1 model, namely radiation heat transfer model, is selected in this study.

Combustion model

At the beginning of the combustion model, fuel and oxidizer are required to enter the cremation furnace with different proportions and air-flow. In this study, a non-premixed combustion model (NPCM) is adopted through the characteristics of cremation. The expression of this model:

$$\frac{\partial}{\partial t}(\rho \bar{f}) + \nabla(\rho \bar{v} \bar{f}) = \nabla \left(\frac{\mu_t}{\sigma_t} \nabla \bar{f} \right) + S_m + S_{\text{user}} \quad (6)$$

$$\frac{\partial}{\partial t}(\rho \bar{f}'^2) + \nabla(\rho \bar{v} \bar{f}'^2) = \nabla \left(\frac{\mu_t}{\sigma_t} \nabla \bar{f}'^2 \right) + C_g \mu_t (\nabla^2 \bar{f}) - C_d \rho \frac{\varepsilon}{k} \bar{f}'^2 + S_{\text{user}} \quad (7)$$

$$f' = f - \bar{f} \quad (8)$$

where S_m is a source from particles of the gas phase or liquid fuel droplets, S_{user} – the user-defined item source, and C_d , μ_t , and C_g – the constant.

In this study, eq. (9) is used to determine the temperature density and substance concentration:

$$\Phi_i = \Phi_i(f, H'') \quad (9)$$

where Φ_i is material concentration, f – the density, and H'' – the temperature.

Mesh generation and numerical solution

The computing domain is constructed by GAMBIT 2.4. To ensure that the grid quality is not affected, the grid adopted in this study is a structured grid. Under the condition of the

computing accuracy, the regions such as burner outlet, secondary tuyere, and furnace outlet are grid-shaped. In the whole computing area, the minimum size of the grid is divided into $2.5 \times 2.5 \times 2.5$ mm, and the maximum size is segmented into $25 \times 25 \times 25$ mm, and the total number of the grid after division is 1623000. Through the independence test of the grid, it is found that the flow field in the furnace is simulated by the number of results generated by the grid.

The boundary conditions are:

- the boundary type of the injection nozzle is mass-flow-inlet,
- the boundary type of primary tuyere is vely-inlet,
- the boundary type of secondary tuyere is vely-inlet,
- the boundary type of the combustion zone is mass-flow-inlet/wall (heat flux varying with time),
- the boundary type of the smoke outlet of the main furnace is pressure-outlet.

In the boundary types, the boundary conditions of the combustion zone are changed with time, thus user-defined functions are written to implement the boundary conditions.

In this study, 0 light diesel oil is mainly used in the process of police cremation, and its chemical composition is shown in tab. 1.

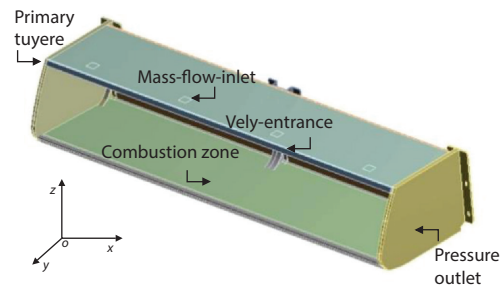


Figure 2. Schematic diagram of computational domain; *primary tuyere: the boundary type of the nozzle is the wind inlet; mass-flow-inlet: the boundary type of the nozzle is the air-flow mass flow; vely-entrance: boundary entry of the primary tuyere; combustion zone: the location where the main furnace produces combustion; pressure outlet: boundary type outlet of main furnace flue gas outlet*

Table 1. Chemical element composition and properties of number 0 light diesel oil

Main burner	Mass [kgh ⁻¹]	M [%]	w(C) [%]	w(H) [%]	w(O) [%]	w(N) [%]	w(S) [%]	A [%]	Net calorific power [Jkg ⁻¹]	Specific heat [Jkg ⁻¹ K ⁻¹]
Number 0 light diesel oil	25	0	85.47	13.52	0.67	0.03	0.27	0.02	4.32 E + 7	2100

According to the statistical results of relevant quantities, the percentage of chemical element composition and related properties of human body and buried goods are shown in tab. 2.

Table 2. Chemical element composition content of incinerator and its properties

Project	Mass [kgh ⁻¹]	M [%]	w(C) [%]	w(H) [%]	w(O) [%]	w(N) [%]	w(S) [%]	A [%]	Net calorific power [Jkg ⁻¹]	Specific heat [Jkg ⁻¹ K ⁻¹]
Human body	65	63	17	2.8	8.35	2	0.28	3.54	-	
Buried objects	5	15	40	6	24	0	0	8		
Admixture	70	60.34	20.15	309	9.43	2.96	0.27	3.63	9.3 E + 6	3200

According to the calculation, the air combustion volume is 19.107 kg. When the excess coefficient of air is set as 1.2, the proportion of air distribution is 90% and the relevant parameters of combustion supporting air distribution are shown in tab. 3.

Table 3. Relevant parameters of combustion wind

Project	Speed [m·s]	Temperature [K]	Density [kgm ⁻³]	Proportion [%]
Primary air	58	320	1.6	85
Secondary air	7	660	0.659	15

To verify the accuracy of the simulation results, the furnace structure under six different working conditions is set. Then the thermocouple section, the temperature, and velocity distribution of the central section of the main furnace are selected to optimize the mechanism of the cremation furnace. The presentence of the furnace structure under six different working conditions is shown in tab. 4.

Table 4. Several common furnace structures

Condition number	Description of furnace structure
1	The burner is placed opposite the door of the furnace, the flue gas outlet is arranged on both sides of the door of the furnace, and the secondary combustion air injection nozzle is set on both sides of the furnace
2	The burner is placed opposite the door of the furnace, and the flue gas outlet is set at the top of the furnace, maintaining the same area as the working Condition 1. The secondary combustion air injection nozzle is set on the upper and lower sides of the furnace
3	No burner is set opposite the door of the furnace, and only the secondary combustion air injection nozzle is arranged on the upper part of the furnace, thus the secondary wind speed becomes twice as before, and then the total amount of secondary wind remains unchanged. Other structures are consistent with working Condition 1.
4	No burner is set opposite the door of the furnace, and only the secondary combustion air injection nozzle is arranged on the upper part of the furnace, thus the secondary wind speed becomes twice as before, and then the total amount of secondary wind remains unchanged. Other structures are consistent with working Condition 1.
5	The burner is placed on the side of the furnace. The center line of this position needs to be one third of the direction close to the furnace door, and it should be 45° with the cremated body. Other structures should be consistent with working Condition 1.
6	The burner is placed on the side of the furnace. The center line of this position needs to be one third of the direction close to the furnace door, and it should be 45° with the cremated body. Other structures should be consistent with working Condition 1.

Results

Model validation results

Before the numerical calculation, the temperature in the cremation furnace was measured by three thermocouples arranged in the fire rate furnace. In the numerical calculation, firstly, the furnace structure is simulated under the condition of working Condition 1, and the simulated temperature results are compared with the actual test data results, as shown in figs. 3 and 4. In the three tests of temperature measuring points, the calculated value of temperature measuring point 1 and temperature measuring point 2 are close to the measured value, while compared with the measured value of temperature measuring point 3, the difference between the calculated value and the measured value is about 100 °C, while the vertical distance between temperature measuring point 3 and the burner is about 5000 mm. Among the three test points, temperature test point 3 is the closest to the burner. When the body enters the furnace, preheating is carried out at the edge of the furnace for 20 min, which is the main reason for

the simulation error. Therefore, the measured temperature of the combustion wind has reached 300 °C. Therefore, in the actual combustion process, when the combustion near test point 3 is very sufficient, during the calculation process, the combustion nearby is not sufficiently ignited. This is confirmed by the distribution of oxygen concentration. The low oxygen concentration is caused by the near distance between combustor. As shown in the simulation and test results that the structure is quite accurate in the process of simulation of the working conditions, especially in the latter part of the furnace, because the outlet is also set in the latter part. Thus, a good guiding significance is provided for experimental design and structural optimization of furnace.

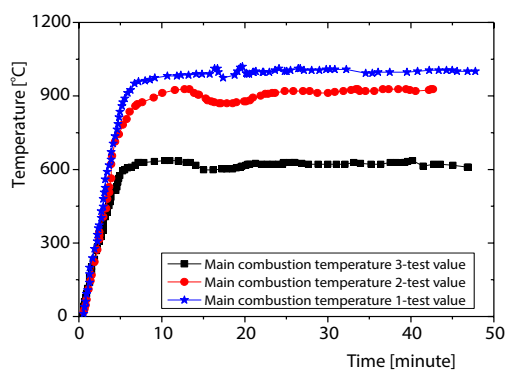


Figure 3. Variation diagram of temperature test value in working Condition 1

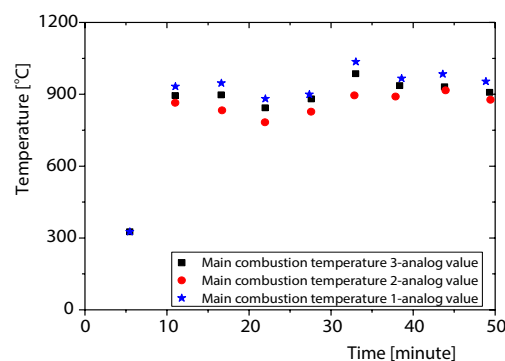


Figure 4. Variation diagram of temperature simulation value in working Condition 1

Comparative optimization analysis of simulated cremation furnace structure

According to the experimental results, and from the perspective of the temperature distribution on the cross-section of the thermocouple, the working condition with a change of 5 is the least ideal working condition. The emission angle is changed, thus the time the fuel stays in the furnace is not enough for complete combustion of remain. Under the conditions of working Conditions 1 and 6, the temperature gradient from outside to inside of the furnace is too large, which is not conducive to the effective combustion of fuel. Therefore, from the perspective of the temperature distribution on the thermocouple cross-section, the structure of working Condition 2 is the best.

From the perspective of the velocity distribution on the thermocouple cross-section, there is no significant difference in the velocity distribution under Condition 2 and Condition 4. In working Conditions 1, 5, and 6, the low speed zone is small, and there is a large flow rate above the body. This phenomenon helps the volatiles and coke produced by the burning body react with the surrounding air as soon as possible.

From the point of view of the temperature distribution on the central section of the furnace, the temperature field on the central section of the furnace is higher under working Conditions 1, 5, and 6, which are favorable for the combustion in the furnace. The other three conditions are relatively poor, not conducive to the full combustion of the body in the furnace.

From the point of view of the distribution of burning speed on the central section of the furnace, there is no difference in the distribution of combustion velocity on the central section of the furnace under different working conditions. Because the incidence angle of the burner is small, the combustion velocity direction from outside to inside in operating situation 5 and 6 is more widely distributed, which is more conducive to the contact between air fuel and

the surface of the body. Because the incidence angle of the burner is small, the combustion velocity direction from outside to inside in operating situation 5 and 6 is more widely distributed, which is more beneficial for the contact between air fuel and the surface of the body.

Discussion

With the evolution of the times, cremation is one of the most popular ways to deal with the dead. To optimize the structure of cremation equipment and promote the use efficiency of incineration equipment, the heat transfer process of cremation furnace is simulated by finite element in this study. At present, there are few analysis for cremator, but more studies for finite element simulation of combustion process. Through the adoption of finite element commercial CFD software, the combustion process of six different particles in a cylindrical combustion chamber is imitated by Mao *et al.* [12]. The temperature of different sections, the coefficient of inhomogeneity, the mass fraction of oxygen, and the mass distribution of nitric oxide in the combustion chamber were analyzed, and the results reveal that the maximum temperature of high calorific value fuel on each section is relatively lower than that of calorific value fuel. According to the relevant parameters of this study, the influence factors of the combustion in the cremation furnace are analyzed, and the combustion temperature and combustion speed are selected to obtain the CFD model established in this study, which can accurately predict the temperature field and velocity field in the cremation furnace. Moreover, the verified numerical model is tested for furnace structure optimization. The appropriate boundary conditions in the corresponding numerical model are limited by Krishnaraj *et al.* [13] to optimize the geometry of the combustion chamber. The 3-D Navier-Stokes equations are adopted to solve the combustion simulation, and the feasibility of the CAE model is determined by using the control equations in the finite element modelling and finite element analysis software. According to the enlightenment of the aforementioned study, six different working situations are set, and the optimal operating circumstances are obtained by using the finite element.

Conclusions

To study the heat transfer in the cremation furnace and design the structure of the cremation furnace reasonably, the finite element simulation method is adopted to simulate the temperature and combustion rate of the cremation furnace. Firstly, the research object and the simplified model is introduced in this study, and the temperature difference and velocity field in the cremation furnace is simulated through Gambit and FLUENT in the commercial CFD software. The flow, heat transfer and combustion model adopted in this study are described, and the CFD model of finite element cremation furnace is established according to the thermodynamic theory model, and the finite element model is meshed and calculated numerically. Experimental results show that the CFD model established in this study can accurately foretell the temperature field and velocity field in the cremation furnace. Moreover, the verified numerical model was examined for the optimization of the furnace structure. The experimental results show that the furnace structure of working Condition 1, 2, and 4 designed in this study is built based on good computation results, and the full combustion of remains is ensured by operating situation 1. The residence time of high temperature flue gas in the furnace and is prolonged by Condition 2, which can make the temperature distribution in the furnace more uniform, and conducive to the full combustion of remains. The highest of the combustion efficiency of the whole furnace is realized by working circumstance 4.

A good theoretical basis for the optimization of cremation equipment structure in China's cremation industry is provided by this study. However, the study still has limitations,

only six working conditions are considered in the process of structural optimization. It is hoped that more working conditions can be considered in subsequent studies, such as the placement of burner, smoke outlet, and other locations, to expand the depth of this study.

Acknowledgment

The General Project Fund of Civil Aviation Flight University of China J2019-029.

References

- [1] Warmlander, S. K. T. S., et al., Estimating the Temperature of Heat – Exposed Bone Via Machine Learning Analysis of Sci Color Values: A Pilot Study, *Journal of Forensic Sciences*, 64 (2019), 1, pp. 190-195
- [2] Sapogin, L. G., et al., The Visual Problem of High Energy Physics, Gravitation and Cosmology, *Global Journal of Science Frontier Research: A Physics and Space Science*, 19 (2019), 2, pp. 1-36
- [3] Sheikholeslami, M., Ghasemi, A., Solidification Heat Transfer of Nanofluid in Existence of Thermal Radiation by Means of FEM, *International Journal of Heat and Mass Transfer*, 123 (2018), Aug., pp. 418-431
- [4] Shaofei, W., Study and Evaluation of Clustering Algorithm for Solubility and Thermodynamic Data of Glycerol Derivatives, *Thermal Science*, 23 (2019), 5A, pp. 2867-2875
- [5] Wang, W. Q., et al., Parallel Finite Element Modelling of Multi-Physical Processes in Thermochemical Energy Storage Devices, *Applied energy*, 185 (2017), Part 2, pp. 1954-1964
- [6] Fang, L., et al., A Computationally Efficient Numerical Model for Heat Transfer Simulation of Deep Borehole Heat Exchangers, *Energy and Buildings*, 167 (2018), May, pp. 79-88
- [7] Lohrasbi, S., et al., Multi-objective RSM Optimization of Finite Assisted Latent Heat Thermal Energy Storage System Based on Solidification Process of Phase Change Material in Presence of Copper Nanoparticles, *Applied Thermal Engineering* 118 (2017), May, pp. 430-447
- [8] Wang, Z. P., et al., Finite Element Thermal Model and Simulation for a Cylindrical Li-Ion Battery, *IEEE Access*, 5 (2017), July, pp. 15372-15379
- [9] Ma, J., et al., Simulation of Combined Conductive, Convective and Radiative Heat Transfer in Moving Irregular Porous Fins by Spectral Element Method, *International Journal of Thermal Sciences*, 118 (2017), Aug., pp. 475-487
- [10] Bilgin, M. B., et al., The 3-D Finite Element Model of Friction Drilling Process in Hot Forming Processes, Proceedings of the Institution of Mechanical Engineers – Part E: *Journal of Process Mechanical Engineering*, 231 (2017), 3, pp. 548-554
- [11] Shaofei, W., A Traffic Motion Object Extraction Algorithm, *International Journal of Bifurcation and Chaos*, 25 (2015), 14, 1540039
- [12] Mao, Y., et al., Numerical Simulation of Combustion of Biomass Pellets Based on Fluent, *Journal of Engineering for Thermal Energy and Power*, 32 (2017), 12, pp. 121-125
- [13] Krishnaraj, J., et al., Combustion Simulation and Emission Prediction of Different Combustion Chamber Geometries Using Finite Element Method, *Materials Today: Proceedings*, 4 (2017), 8, pp. 7903-7910